The Role of Autophagy in the Innate Immune Response to Fungal Keratitis Caused by *Aspergillus fumigatus* Infection

Chenyu Li, Cui Li, Jing Lin, Guiqiu Zhao, Qiang Xu, Nan Jiang, Qian Wang, Xudong Peng, Guoqiang Zhu, and Jiaqian Jiang

Department of Ophthalmology, the Affiliated Hospital of Qingdao University, Qingdao, Shandong Province, China

Correspondence: Guiqiu Zhao, Department of Ophthalmology, the Affiliated Hospital of Qingdao University, 16 Jiangsu Road, Qingdao, Shandong Province, China; zhaoguiqiu_good@126.com.

CL and CL are co–first authors.

Received: March 23, 2019
Accepted: October 30, 2019
Published: February 21, 2020

Citation: Li C, Li C, Lin J, et al. The role of autophagy in the innate immune response to fungal keratitis caused by *Aspergillus fumigatus* infection. *Invest Ophthalmol Vis Sci.* 2020;61(2):25. https://doi.org/10.1167/iovs.61.2.25

Purpose. To determine the role of autophagy in the innate immune response to fungal keratitis (FK) caused by *Aspergillus fumigatus* infection.

Methods. Corneal samples obtained from patients and mice with FK were visualized via transmission electron microscopy (TEM). Autophagy-related proteins LC3B-II, Beclin-1, LAMP-1, and p62 in *A. fumigatus*-infected corneas of C57BL/6 mice were tested by Western blot. After treatment with autophagy inhibitors 3-methyladenine (3-MA), chloroquine (CQ), or inducer rapamycin, autophagy-related proteins were detected by Western blot. Corneas were photographed with slit lamp microscopy and pathological changes were observed by hematoxylin and eosin staining. Polymorphonuclear neutrophilic leukocytes (PMNs) were assessed by immunofluorescent staining and observed under TEM. The levels of CXCL-1, IL-1β, HMGB1, IL-18, TNF-α, and IL-10 were tested by reverse transcription polymerase chain reaction and Western blot. The quantification of fungal loads was detected and photographed.

Results. The accumulation of autophagosomes in corneas of patients and mice with FK was observed with TEM. The expression of LC3B-II, Beclin-1, and LAMP-1 was elevated in corneas after fungal infection, whereas p62 was reduced. Treatment with 3-MA or CQ upregulated clinical scores, pathological changes, and the expression of CXCL-1, IL-1β, HMGB1, IL-18, and TNF-α except IL-10. The morphology of PMNs was changed and PMN recruitment was increased in mice corneas treated with 3-MA or CQ, whereas rapamycin reduced the inflammatory response to keratitis. These results were statistically significant.

Conclusions. *A. fumigatus* infection increases the expression of autophagy in corneas. Autophagy plays an anti-inflammatory role in the innate immune response to *A. fumigatus* keratitis.

Keywords: fungal keratitis, *Aspergillus fumigatus*, autophagy

Fungal keratitis (FK), a serious ocular disease caused by fungal pathogens infection, is one of the principal causes of blindness in developing countries.[1] Increased corneal injury, especially agricultural trauma, excessive use of corticosteroids and long-term usage of antibiotics gradually increase the incidence of this disease.[2] The treatment of FK remains challenging because of the lack of effective medical and surgical treatment.[3] Numerous researches focus on the pathogenesis mechanism of FK to find effective prevention and treatment of FK.[4,5]

Autophagy is a lysosome-mediated degradation process, which regulates intracellular homeostasis of eukaryotes by mediating the degradation of proteins and organelles.[6] Macroautophagy (hereinafter referred to as autophagy) segregates long-lived proteins and bulky cytoplasmic contents within double-bilayer autophagosomes, and delivers them to lysosomes for degradation.[7] It can be significantly activated in response to starvation, stress, hypoxia, tumor, and infection.[8] Autophagy is proved to be a crucial player in immune responses. An increasing number of studies have shown that autophagy can decrease the vulnerability to infection, clear intracellular pathogens, and function in antigen presentation.[9–11] A previous study indicates that autophagy maintains the cellular and immune homeostasis during the *Candida albicans* infection.[12] Autophagy can regulate IL-1β release in human primary macrophage to resist the fungal infection.[13]

In recent years, more and more studies have explored the role of autophagy in the pathogenesis of ocular diseases. Autophagy enhanced the ability to clear *Toxoplasma gondii* and herpes simplex virus of ocular infections.[14] Intravitreal injection of 3-methyladenine (3-MA) reduced the death of retinal ganglion cell in rat models of chronic hypertensive glaucoma, and upregulation of autophagy attenuated the degeneration of retinal ganglion cell after optic nerve severance in mice.[15] In addition, rapamycin increased LC3-II levels in models of uveitis by intraperitoneal injection of lipopolysaccharide (LPS), exerting neuroprotective effects

Copyright 2020 The Authors

This work is licensed under a Creative Commons Attribution-NonCommercial-NoDerivatives 4.0 International License.

and maintaining visual function.[16] Autophagy may play a part in the formation of drusen in aged mice and age-related macular degeneration patients.

However, the function of autophagy in *Aspergillus fumigatus* keratitis is still unknown. In this article, we established murine models of *A. fumigatus* keratitis with or without treatment with phosphoinositide 3-kinase (PI3K) inhibitor 3-MA, late autophagy inhibitor chloroquine (CQ), or mammalian target of rapamycin inhibitor, which are commonly used to inhibit or induce autophagy, to describe the expression and the role of autophagy in the innate immune response to mice with *A. fumigatus* keratitis.

Materials and Methods

Corneal Samples of Patients with FK

A total of 20 cornea samples of patients with FK (*Fusarium* 9, *Aspergillus* infection 11; aged 40–70 years) and remaining tissues of 20 healthy donors used for keratoplasty were collected as control groups. The corneas were preserved into 2.5% glutaraldehyde (Solarbio, Beijing, China) for 2 minutes, preparing for examination by transmission electron microscopy (TEM). The protocol for the research abide by the provisions of the Declaration of Helsinki in 1995 (as revised in Edinburgh 2000). Patients consented to the management of samples, and the experiment was approved by the Institutional Research Ethics Committee at the Affiliated Hospital of Qingdao University.

Preparation of *A. fumigatus*

A. fumigatus strain 3.0772 was bought from China General Microbiological Culture Collection Center (Beijing, China) and cultured in Sabouraud medium for 5 to 7 days. After being shaken in Sabouraud liquid medium for 3 days, *A. fumigatus* was collected and separated into 20 to 40 µm fractions. Fungal fractions were washed with sterile phosphate-buffered saline (PBS) and centrifuged three times. Then the liquid supernatant was discarded. Dulbecco's Modified Eagle's Medium (DMEM; Gibco, San Diego, CA, USA) was added into *A. fumigatus* and yielded 1×10^8 CFU/mL.

Murine Model of FK

Specific pathogen-free C57BL/6 mice (female, 8 weeks) were purchased from Changzhou Cavens Laboratory Animal Co., Ltd. (Jiangsu, China). The animals were treated according to the Statement for the Use of Animals in Ophthalmic and Vision Research made by the ARVO. The left corneas of mice were chosen as experimental group and infected by routine method.[4] Six scraped corneas were randomly selected as sham-operation group without infection. The right eyes were used as normal control eyes. Mice corneas were obtained at 12 hours, 1 day, and 3 days postinfection (p.i.). The standard of clinical scoring referred to Wu et al.[17] The total score of 5 or less was mild, 6 to 9 was moderate, and over 9 was severe.

3-MA, CQ, and Rapamycin Treatment of Murine Model

Autophagy inhibitor 3-MA (Sigma, St. Louis, MO, USA) dissolved in dimethyl sulfoxide (DMSO) was diluted with PBS to a concentration of 15 µg/5 µL, and then subconjunctivally injected into the left eyes of C57BL/6 mice. Additional 3-MA (300 µg/100 µL) was injected intraperitoneally 1 day p.i.[18] CQ (Sigma) was given to mice by subconjunctival injections (25 µg/5 µL) 1 day before infection and intraperitoneal injections (500 µg/100 µL) 1 day p.i.[19] Infected controls were similarly injected with DMSO or PBS. Mice were injected subconjunctivally (0.5 µg/5 µL) with autophagy inducer rapamycin (MCE, Princeton, NJ, USA) 1 day before infection and injected intraperitoneally (120 µg/100 µL) 1 day p.i. The vehicle group was injected with PBS containing 3% alcohol and 5% Tween-80 (Solarbio) 1 day before infection and injected intraperitoneally 1 day p.i. as infected control group.[20] The corneas were collected at 3 days for reverse transcription polymerase chain reaction (RT-PCR) and Western blot. Eyeballs were removed at 3 days for observation with fluorescence microscopy and hematoxylin and eosin (H&E) staining.

Transmission Electron Microscopy

Corneal tissue samples from patients with FK, healthy donors, and mice (n = 6/group/time) with or without *A. fumigatus* infection were fixed with 2.5% glutaraldehyde at 4°C for 3 days. Experimental procedures for preparation of corneal sample observed by TEM were performed according to routine methods.[21] Autophagosomes and polymorphonuclear neutrophilic leukocytes (PMNs) were examined and photographed under a TEM. The absolute number of autophagosomes and granules in each cell was counted, and the definition of euchromatin fraction was based on previous studies.[22]

Western Blot Analysis

Mice corneas (n = 6/group/time) were harvested at 3 days p.i. Protein extraction and concentration determination were performed as described previously.[4] The protein was separated on 12% acrylamide SDS-PAGE and transferred to polyvinylidene difluoride (PVDF; Solarbio) membrane. Membranes were washed in PBS containing 0.05% Tween-20 (Bio-Rad, Hercules, CA, USA) (PBST) three times. After being blocked with blocking buffer (Beyotime, Jiangsu, China) at 37°C for 2 hours, the membrane was incubated with antibodies to GAPDH (1:1000; Elabscience, Wuhan, China), CXCL-1 (1:1000; Affinity Biosciences, Jiangsu, China), LC3B (1:1000; Cell Signaling Technology, Danvers, MA, USA), SQSTM1/p62 (1:1000; Cell Signaling Technology), Beclin-1 (1:1000; Cell Signaling Technology), LAMP-1 (1:1000; Cell Signaling Technology), IL-1β (1:1000; NOVUS, Littleton, CO, USA), IL-18 (1:500; Abcam, Cambridge, MA, USA), HMGB1 (1:1000; Abcam), TNF-α (1:2000; Proteintech Group, Wuhan, China), or IL-10 (1:1000; Abcam) at 4°C overnight. Membranes were washed in PBS containing 0.05% Tween-20 (Bio-Rad, Hercules, CA, USA) (PBST) three times. Membranes were incubated with corresponding peroxidase-conjugated secondary antibodies (1:5000; Santa Cruz Biotechnology, Santa Cruz, CA, USA) at 37°C for 1 hour. Membranes were developed by chemiluminescence (ECL; Thermo Fisher Scientific, Waltham, MA, USA).

Immunofluorescent Staining

The eyeballs of mice (n = 6/group/time) were removed and frozen rapidly in optimal cutting temperature compound (O.C.T.; SAKURA Tissue-Tek, Torrance, CA, USA) by liquid nitrogen. A total of 10 µm slices were fixed in acetone for

Investigative Ophthalmology & Visual Science

Table. Primer List Used for RT-PCR

Gene	GenBank No.	Primer Sequence (5'-3')
β-actin	NM_007393.3	F: GATTACTGCTCTGGCTCCTAG C
		R: GACTCATCGTACTCCTGCTTGC
CXCL-1	NM_008176.3	F: TGC ACC CAAACC GAA GTC
		R: GTC AGAAGC CAG CGT TCA CC
TNF-α	NM_013693.2	F: ACCCTCACACTCAGATCATCTT
		R: GGTTGTCTTTGAGATCCATGC
IL-1β	NM_008361.3	F:CGCAGCAGCACATCAACAAGAGC
		R:TGTCCTCATCCTGGAAGGTCCACG
HMGB1	NM-000071.6	F: GGCGAGCATCCTGGCTTATC
		R: GGCTGCTTGTCATCTGCTG
IL-18	NM_008360.2	F: GCCTGTGTTCGAGGATATGACTGA
		R: TTCACAGAGAGGGTCACAGCCA
IL-10	NM_010548.2	F: TGCTAACCGACTCCTTAATGCAGGAC
		R: CCTTGATTTCTGGGCCATGCTTCTC

5 minutes and washed with PBS. The slices were blocked with 10% blocking goat serum (Solarbio) at 37°C for 30 minutes. The slices were incubated with rat anti-mouse NIMP-R14 (1:200; Santa Cruz Biotechnology, Inc., Santa Cruz, CA, USA) at 4°C overnight, and then washed with PBS. After being stained with fluorescein isothiocyanate–conjugated goat anti-rat antibody (1:100; Bioss, Beijing, China) for 1 hour and with DAPI for 10 minutes, the slices were photographed by fluorescence microscope and confocal microscopy. The number of neutrophil fluorescent spots in each corneal tissue were counted.

H&E Staining

The eyeballs (n = 6/group/time) were fixed in 4% paraformaldehyde at 4°C for 3 days and then removed the lens. The eyeballs were embedded in paraffin and were filleted under cryostat. The slices were stained according to routine methods[23] and photographed under a light microscopy.

Real-Time RT-PCR

Mice (n = 6/group/time) were euthanized at 3 days p.i. Experimental procedures for RNA extraction, concentration determination, reverse transcription, and RT-PCR reaction were performed as described previously.[4] The primer pair sequences used in this study are shown in the Table.

Quantification of Fungal Loads

Corneas of mice (n = 6/group/time) were harvested at 3 days p.i. Each cornea was ground and diluted with 500 µL PBS, and then cultured in Sabouraud medium at 37°C for 2 days. Colonies were counted according to the previous methods.[24] Results are shown as CFU (10^3)/mL.

Statistical Analysis

The statistical test used was 1-way ANOVA with post hoc least-significant difference *t*-test. Data in this study were shown as the mean ± SEM and considered to be significant at $P \leq 0.05$. Images of Western blot and nuclear euchromatin fraction were analyzed by Image J (National Institutes of Health, Bethesda, MD, USA) according to a previous study.[22] The number of neutrophil fluorescent spots were counted using Image-Pro Plus 6.0 (Media Cybernetics, Inc., Rockville, MD, USA). Statistical analysis and charting were performed with GraphPad Prism 5 (GraphPad Software, San Diego, CA, USA). The images in this study were processed by Adobe Photoshop CS6 (Adobe, San Jose, CA, USA) for aesthetics with the authenticity assured. All experiments were repeated twice to ensure the credibility.

Results

Autophagosome Formation in Corneas of Patients with FK and Mice after *A. fumigatus* Infection

TEM images showed that autophagosomes were not present in the cornea of healthy donors (Fig. 1A). The cornea of patients with FK increased the accumulation of autophagosomes with double-bilayer membranes in the cytoplasm. Digested and degraded substances were present inside the bodies (Fig. 1B). Next, we tested the expression of autophagy-related proteins in corneas of mice after fungal infection. Photographs taken by a slit lamp showed an obviously elevated disease severity assessed by clinical scores at 12 hours, 1 day, and 3 days p.i. Clinical scores were shown in Figure 1F. Compared with sham-operation group, results of Western blot demonstrated that *A. fumigatus* infection gradually increased the expression of LC3B-II (Fig. 1G; $P < 0.001$, $P < 0.001$, $P < 0.001$), LAMP-1 (Fig. 1I; $P < 0.01$, $P < 0.001$, $P < 0.01$), and Beclin-1 (Fig. 1J; $P < 0.001$, $P < 0.001$, $P < 0.001$) in corneas of mice at 12 hours, 1 day, and 3 days p.i. However, the protein level of p62 (Fig. 1H; $P < 0.001$, $P < 0.001$, $P < 0.001$) was gradually decreased at 12 hours, 1 day, and 3 days p.i. To confirm these data, we observed the accumulation of autophagosomes in corneas of mice at 3 days p.i. Photographs showed that *A. fumigatus* infection (Fig. 1L) increased the formation of autophagosomes in the cytoplasm in mice corneas when compared with normal group (Fig. 1K). Multiple vesicular bodies with double-bilayer membranes containing digested and degraded substances were observed in corneas after *A. fumigatus* infection.

Effect of Autophagy on Clinical Score and Pathology

To evaluate the role of autophagy in disease response and pathology, we detected disease severity with slit lamp and pathology with H&E staining in mice corneas treated with 3-MA, CQ, or rapamycin at 3 days p.i. Results showed that corneal edema and opacity were more severe in corneas after 3-MA treatment (Fig. 2B) than in DMSO control group (Fig. 2A; $P < 0.05$). Clinical score was higher in corneas after CQ treatment (Fig. 2D) versus PBS control group (Fig. 2C; $P < 0.05$). However, rapamycin treatment (Fig. 2J) significantly reduced the corneal manifestation compared with the infected group (Fig. 2I; $P < 0.01$). Consistent with the clinical scores, results of pathology manifested higher severity of ulcer and larger number of inflammatory cells in corneas after 3-MA treatment (Fig. 2F) versus DMSO control corneas (Fig. 2E). Pathological changes were significantly aggravated in corneas after CQ treatment (Fig. 2H) compared with PBS control group (Fig. 2G). Treatment with rapamycin (Fig. 2M) alleviated the corneal pathological changes when compared with the infected corneas (Fig. 2L). There was no significant difference in clinical scores (Fig. 2K) and pathological changes (Fig. 2N) between *A. fumigatus* infected corneas and each infected

Investigative Ophthalmology & Visual Science

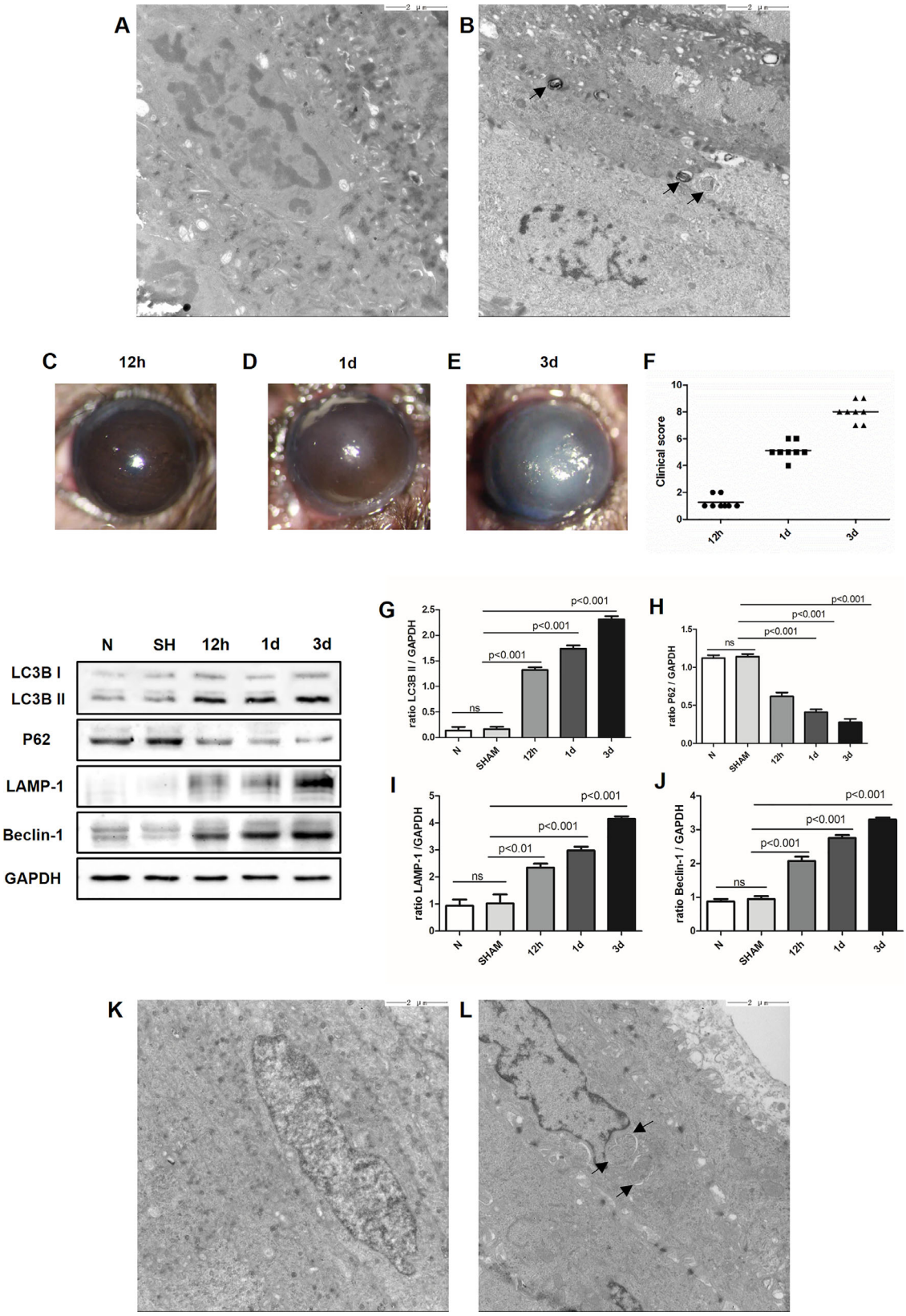

Figure 1. Autophagosome formation in corneas of patients with FK and mice after *A. fumigatus* (marked as AF in figures) infection. (**A-B**) TEM images of autophagosomes in corneas of healthy donors and patients with FK. Arrows indicate autophagosomes; (**C-E**) Infected corneas of C57BL/6 mice at 12 hours, 1 day, and 3 days p.i.; (**F**) Clinical scores are shown as mean ± SEM. Each symbol represents an individual mouse; (**G-J**) Protein levels of LC3B-II, p62, LAMP-1, and Beclin-1 in corneas of C57BL/6 mice after 12 hours, 1 day, and 3 days p.i. Quantitation of proteins is shown as mean ± SEM; (**K-L**) TEM images of autophagosomes in normal and infected corneas of C57BL/6 mice. Arrows indicate autophagosomes. Results revealed that the accumulation of autophagosomes was increased in corneas of human and mice with FK.

Investigative Ophthalmology & Visual Science

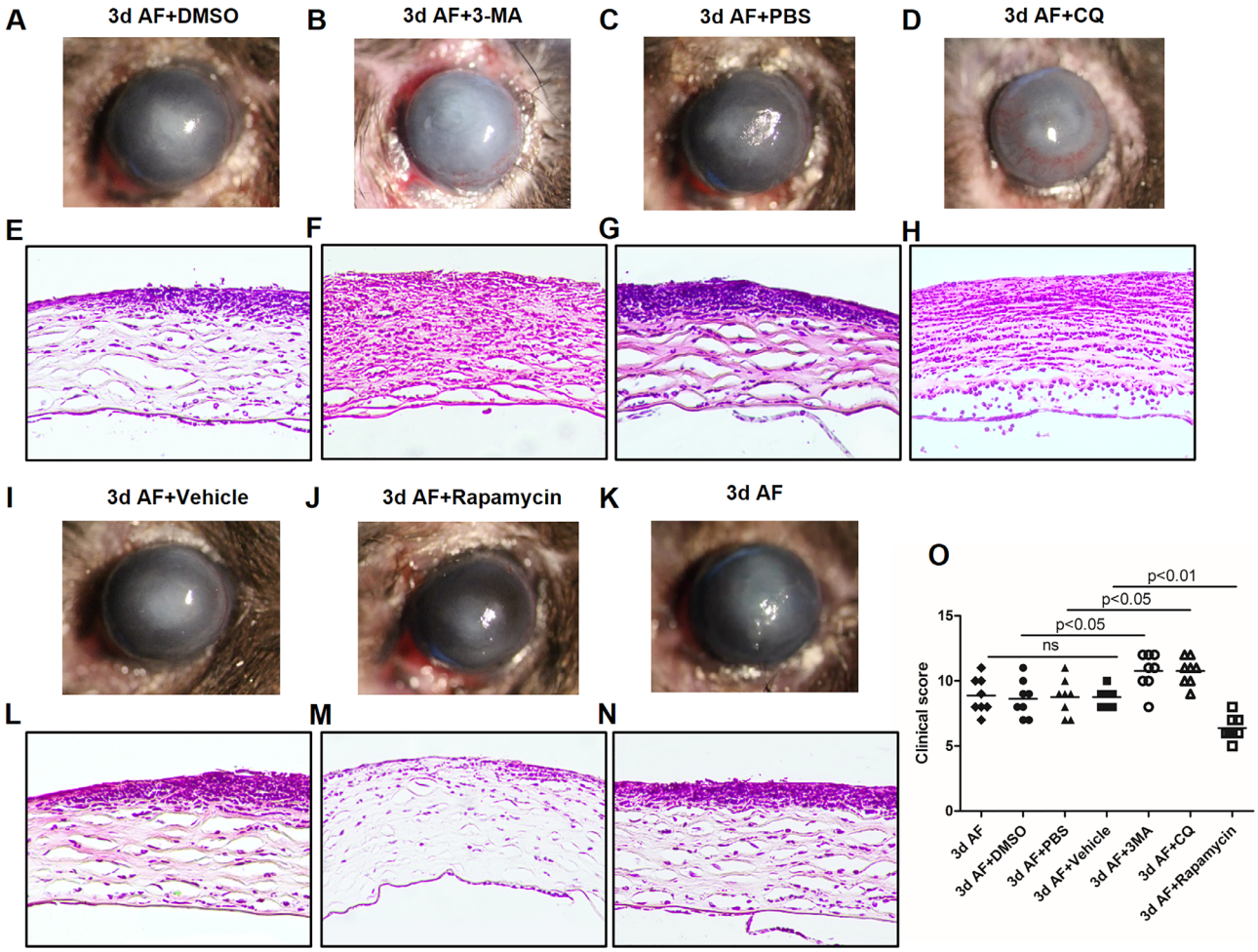

Figure 2. Effect of autophagy on clinical score and pathology. (**A-B**) Infected corneas of C57BL/6 mice after 3-MA or DMSO treatment; (**C-D**) Infected corneas of C57BL/6 mice after CQ or PBS treatment; (**E-F**) Pathological changes in corneas of C57BL/6 mice after 3-MA or DMSO treatment; (**G-H**) Pathological changes in corneas of C57BL/6 mice after CQ or PBS treatment; (**I-J**) Infected corneas of C57BL/6 mice after rapamycin or infected control treatment; (**K**) Infected corneas of C57BL/6 mice at 3 days p.i.; (**L-M**) Pathological changes in corneas of C57BL/6 mice after rapamycin or infected control treatment; (**N**) Pathological changes in corneas of C57BL/6 mice at 3 days p.i.; (**O**) Clinical scores are shown as mean ± SEM. Each symbol represents an individual mouse. Treatment with 3-MA and CQ increased the clinical scores and pathological changes in infected corneas compared with infected control group, whereas rapamycin alleviated disease severity. Magnification (**E-H**, **L-N**): × 200.

control groups separately. Clinical scores are shown in Figure 2O.

Expression of Autophagy-Related Proteins in Corneas of C57BL/6 Mice after 3-MA, CQ, and Rapamycin Treatment

To evaluate the effects of 3-MA, CQ, and rapamycin on autophagy, we examined the expression of autophagy-related proteins by Western blotting. The results indicated that the expression of LC3B-II (Fig. 3A; $P < 0.05$), LAMP-1 (Fig. 3C; $P < 0.05$), and Beclin-1 (Fig. 3D; $P < 0.01$) was reduced, and the expression of p62 (Fig. 3B; $P < 0.05$) was upregulated in 3-MA-treated corneas compared with DMSO control corneas at 3 days p.i. Treatment with CQ increased the expression of LC3B-II (Fig. 3E; $P < 0.01$), LAMP-1 (Fig. 3G; $P < 0.05$), Beclin-1 (Fig. 3H; $P < 0.01$), and p62 (Fig. 3F; $P < 0.01$) when compared with PBS control group at 3 days p.i. In contrast to the results of 3-MA treatment, higher expression of LC3B-II (Fig. 3I; $P < 0.01$), LAMP-1 (Fig. 3K; $P < 0.01$), Beclin-1 (Fig. 3L; $P < 0.01$) and lower expression of p62 (Fig. 3J; $P < 0.001$) were detected in rapamycin-treated corneas versus infected control group.

Effect of Autophagy on PMN Recruitment and Morphology in Corneas after *A. fumigatus* Infection

The mRNA and protein levels of CXCL-1, which plays an important role in the recruitment of PMNs, were detected in corneas after 3-MA, CQ, and rapamycin treatment at 3 days p.i. Results investigated that the relative mRNA level of CXCL-1 was elevated in corneas after 3-MA (Fig. 4A; $P < 0.01$) and CQ (Fig. 4B; $P < 0.05$) treatment compared with infected control group at 3 days p.i. Rapamycin decreased the mRNA level of CXCL-1 in mice corneas (Fig. 4C; $P < 0.001$). The protein level of CXCL-1 was also increased in corneas treated with 3-MA (Fig. 4D; $P < 0.05$) or CQ (Fig. 4E;

Investigative Ophthalmology & Visual Science

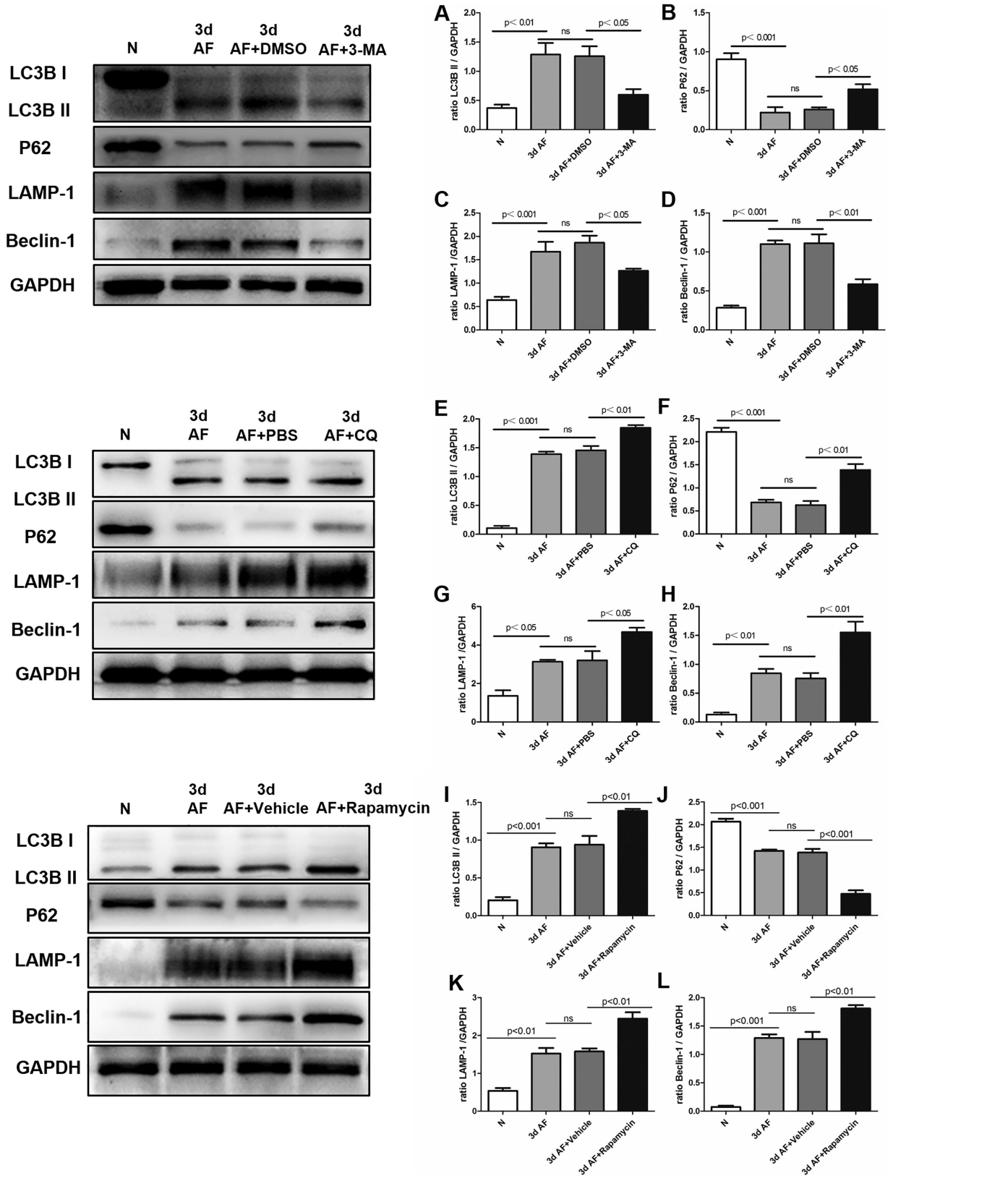

Figure 3. Expression of autophagy-related proteins in corneas of C57BL/6 mice after 3-MA, CQ, and rapamycin treatment. (**A-D**) The protein levels of LC3B-II, p62, LAMP-1, and Beclin-1 in corneas of C57BL/6 mice after 3-MA treatment at 3 days p.i; (**E-H**) The protein levels of LC3B-II, p62, LAMP-1, and Beclin-1 in corneas of C57BL/6 mice after CQ treatment at 3 days p.i; (**I-L**) The protein levels of LC3B-II, p62, LAMP-1, and Beclin-1 in corneas of C57BL/6 mice after rapamycin treatment at 3 days p.i. Quantitation of proteins is shown as mean ± SEM.

Investigative Ophthalmology & Visual Science

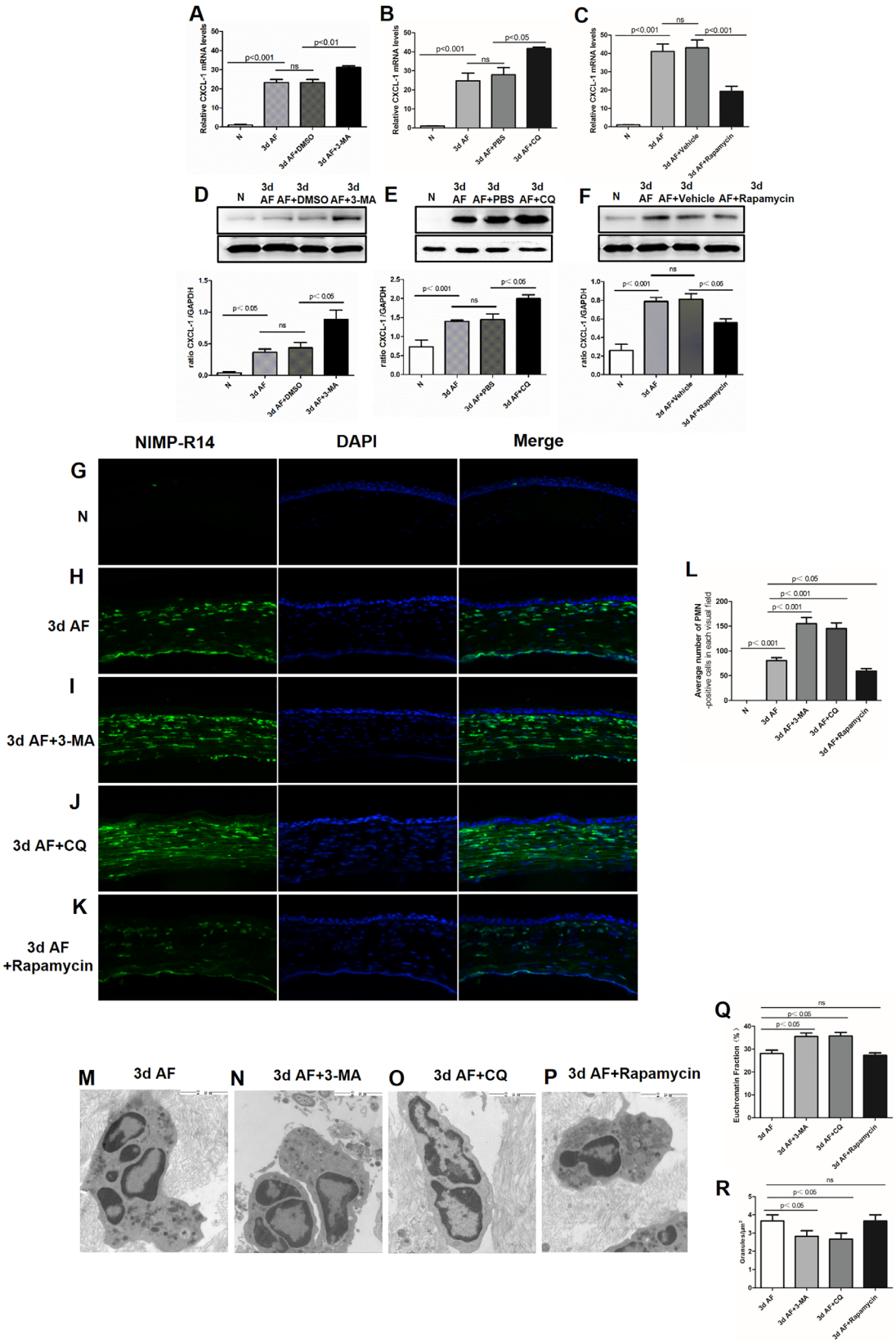

Figure 4. Effect of autophagy on PMN recruitment and morphology. (**A-C**) The mRNA levels of CXCL-1 in corneas of C57BL/6 mice after 3-MA, CQ, or rapamycin treatment at 3 days p.i.; (**D-F**) The protein level of CXCL-1 in corneas of C57BL/6 mice after 3-MA, CQ, or rapamycin treatment at 3 days p.i.; (**G-K**) The fluorescence of PMNs (green) in normal and infected corneas of C57BL/6 mice after treatment with or without 3-MA, CQ, and rapamycin at 3 days p.i.; (**L**) Quantitation of PMNs is shown as mean ± SEM; (**M-P**) TEM images of PMNs morphology in corneas after treatment with or without 3-MA, CQ, and rapamycin at 3 days p.i.; (**Q**) Quantitation of euchromatin fraction of the nucleus is shown as mean ± SEM.; (**R**) Quantitation of granules per cytoplasm area is shown as mean ± SEM. Results indicated that autophagy reduced the production of CXCL-1 and inhibited the recruitment of PMNs in corneas at 3 days p.i. Autophagy inhibition changed the morphology of PMNs in mice corneas after *A. fumigatus* infection. Magnification (**E-I**): × 200.

$P < 0.05$), and reduced in corneas after rapamycin treatment (Fig. 4F; $P < 0.05$) when compared with the infected group at 3 days p.i. Based on these results, immunofluorescence staining was used to confirm the effect of autophagy on PMN recruitment. Data showed that *A. fumigatus* infection after 3 days (Fig. 4H) elevated the number of PMNs when compared with normal corneas (Fig. 4G; $P < 0.001$). After treatment with 3-MA (Fig. 4I; $P < 0.001$) and CQ (Fig. 4J; $P < 0.001$), the number of PMNs was significantly increased in corneas compared with infected control corneas at 3 days p.i. On the contrary, rapamycin (Fig. 4K; $P < 0.05$) can reduce the number of PMNs in corneas after fungal infection. Statistical analysis of PMN fluorescence staining is shown in Fig. 4L. To further detect the effect of autophagy on PMNs, we used TEM to observe the morphology of PMNs. Results of TEM suggested that inhibition of autophagy with 3-MA (Fig. 4N) or CQ (Fig. 4O) increased the euchromatin fraction of the nucleus (Fig. 4Q; $P < 0.05$) and reduced the number of granules per cytoplasm area (Fig. 4R; $P < 0.05$) at 3 days p.i. when compared with infected control corneas (Fig. 4M). In addition, there was no significant difference between rapamycin treatment group (Fig. 4P) and infected control group.

Effects of Autophagy on Inflammatory Factors in *A. fumigatus*-Infected Corneas

To investigate the effect of autophagy on inflammatory factors in corneas after *A. fumigatus* infection, we tested the relative mRNA levels of HMGB1, IL-1β, IL-18, TNF-α, and IL-10 in corneas after 3-MA, CQ, and rapamycin treatment. The results indicated that the relative mRNA expression of IL-1β (Fig. 5A; $P < 0.05$), HMGB1 (Fig. 5B; $P < 0.05$), IL-18 (Fig. 5C; $P < 0.01$), and TNF-α (Fig. 5D; $P < 0.05$) was significantly higher in 3-MA-treated corneas than in DMSO control group at 3 days p.i., whereas the relative mRNA expression of IL-10 was lower after 3-MA treatment (Fig. 5E; $P < 0.05$). In line with the results of 3-MA treatment, CQ increased the relative mRNA levels of IL-1β (Fig. 5F; $P < 0.05$), HMGB1 (Fig. 5G; $P < 0.05$), IL-18 (Fig. 5H; $P < 0.05$), and TNF-α (Fig. 5I; $P < 0.05$) and reduced the relative mRNA level of IL-10 (Fig. 5J; $P < 0.01$) when compared with PBS control group at 3 days p.i. However, the relative mRNA levels of IL-1β (Fig. 5K; $P < 0.001$), HMGB1 (Fig. 5L; $P < 0.001$), IL-18 (Fig. 5M; $P < 0.01$), and TNF-α (Fig. 5N; $P < 0.01$) were downregulated, and the production of IL-10 (Fig. 5O; $P < 0.05$) was enhanced in rapamycin-treated corneas compared with infected control group. To confirm the results of mRNA levels, inflammatory cytokines were examined by Western blot. Higher protein expression of IL-1β (Fig. 6A; $P < 0.001$), HMGB1 (Fig. 6B; $P < 0.05$), IL-18 (Fig. 6C; $P < 0.05$), and TNF-α (Fig. 6D; $P < 0.01$) and lower expression of IL-10 (Fig. 6E; $P < 0.01$) were detected in 3-MA-treated corneas than in DMSO control group at 3 days p.i. CQ treatment increased the protein levels of IL-1β (Fig. 6F; $P < 0.01$), HMGB1 (Fig. 6G; $P < 0.01$), IL-18 (Fig. 6H; $P < 0.01$), and TNF-α (Fig. 6I; $P < 0.05$) and reduced the protein level of IL-10 (Fig. 6J; $P < 0.05$) compared with PBS control group at 3 days p.i. On the contrary, the protein levels of IL-1β (Fig. 6K; $P < 0.05$), HMGB1 (Fig. 6L; $P < 0.05$), IL-18 (Fig. 6M; $P < 0.01$), and TNF-α (Fig. 6N; $P < 0.05$) were downregulated, and the production of IL-10 (Fig. 6O; $P < 0.05$) was elevated in rapamycin-treated corneas compared with infected control group.

Effects of Autophagy on Fungal Loads in *A. fumigatus*-Infected Corneas

We detected the quantification of fungal loads in mice corneas after 3-MA, CQ, and rapamycin treatment. Results showed that the quantification of fungal loads was significantly higher in mice corneas after 3-MA (Fig. 7; $P < 0.05$) treatment than infected control group at 3 days p.i., whereas CQ (Fig. 7; $P < 0.05$) and rapamycin (Fig. 7; $P < 0.05$) decreased the quantification of fungal loads compared with infected control group.

Discussion

Autophagy, which regulates the intracellular homeostasis of eukaryotes, is emerging as a crucial player in immune responses. The defects of autophagy are associated with neurodegeneration, aging, metabolic syndrome, and inflammatory disorders.[25] The TEM results presented in this study revealed that the accumulation of autophagosomes was increased in corneas of patients with FK compared with healthy donors. Next, we established *A. fumigatus* keratitis models to further determine the expression of autophagy. Results showed that *A. fumigatus* infection gradually increased the expression of autophagy-related proteins LC3B-II, Beclin-1, and LAMP-1 and reduced the level of p62 in corneas at 12 hours, 1 day, and 3 days, indicating that the expression of autophagy was highest in corneas at 3 days p.i. To confirm these data, corneas infected with *A. fumigatus* for 3 days were observed with TEM. We observed the accumulation of autophagosomes was significantly enhanced compared with normal mice corneas, showing that *A. fumigatus* infection elevated the level of autophagy in corneas of mice. Our findings are consistent with the previous studies in murine models of acute kidney injury, indicating that the expression of autophagy is rapidly increased after LPS infection.[26] Our results are also consistent with previous studies demonstrating that the accumulation of autophagy is elevated to regulate the release of inflammatory factors in human primary macrophage to resist *A. fumigatus* infections.[13] These data suggest that autophagy may play a potential role in corneas with *A. fumigatus* infection.

Previous studies indicated that autophagy, along with other innate immune responses activation, represents the first line of defense against pathogen infection.[27] It can lead to decreased susceptibility to infection, clear intracellular pathogens and function in antigen presentation.[28] To determine the role of autophagy in *A. fumigatus* keratitis, corneas were injected with autophagy inhibitors 3-MA and CQ. Results showed that 3-MA decreased the accumulation of LC3B-II, Beclin-1, and LAMP-1 and upregulated the level of p62 in corneas of mice after *A. fumigatus* infection, indicating that 3-MA effectively reduced the formation of autophagosomes by inhibiting PI3K. CQ decreased autophagy flux by inhibiting autophagosome fused with lysosome resulting in elevated levels of LC3B-II, Beclin-1, LAMP-1, and p62. Autophagy inducer rapamycin was also injected into corneas. Higher expression of proteins LC3B-II, Beclin-1, and LAMP-1 and lower expression of p62 were observed in corneas with rapamycin treatment versus infected control group, which suggested that rapamycin effectively induced the formation of autophagosomes.

Consistent with the observations that autophagy has an effect on inflammation and pathology in irritable bowel disease and ischemic limb muscle myopathy,[29,30] inhibition

Investigative Ophthalmology & Visual Science

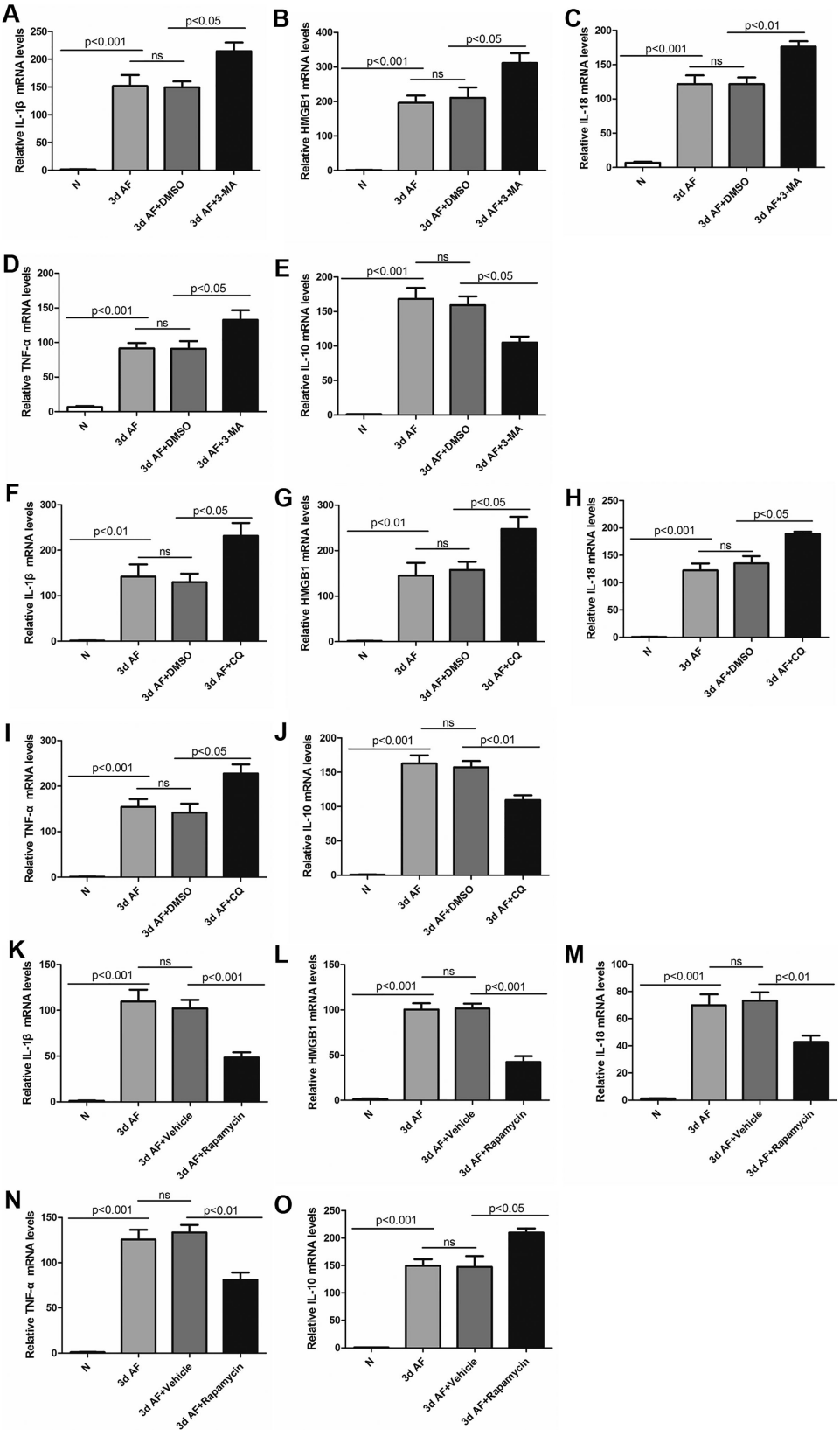

Figure 5. Effect of autophagy on inflammatory factor relative mRNA levels in corneas after *A. fumigatus* infection. (**A-E**) The mRNA levels of IL-1β, HMGB1, IL-18, TNF-α, and IL-10 in corneas of C57BL/6 mice after 3-MA treatment at 3 days p.i.; (**F-J**) The mRNA levels of IL-1β, HMGB1, IL-18, TNF-α, and IL-10 in corneas of C57BL/6 mice after CQ treatment at 3 days p.i.; (**K-O**) The mRNA levels of IL-1β, HMGB1, IL-18, TNF-α, and IL-10 in corneas of C57BL/6 mice after rapamycin treatment at 3 days p.i. 3-MA and CQ enhanced the expression of IL-1β, HMGB1, IL-18, and TNF-α, and reduced the level of IL-10 in corneas compared with infected control group, whereas rapamycin decreased the production of IL-1β, HMGB1, IL-18, and TNF-α, and increased the expression of IL-10 in infected corneas. Quantitation of mRNA levels is shown as mean $\pm$ SEM.

Investigative Ophthalmology & Visual Science

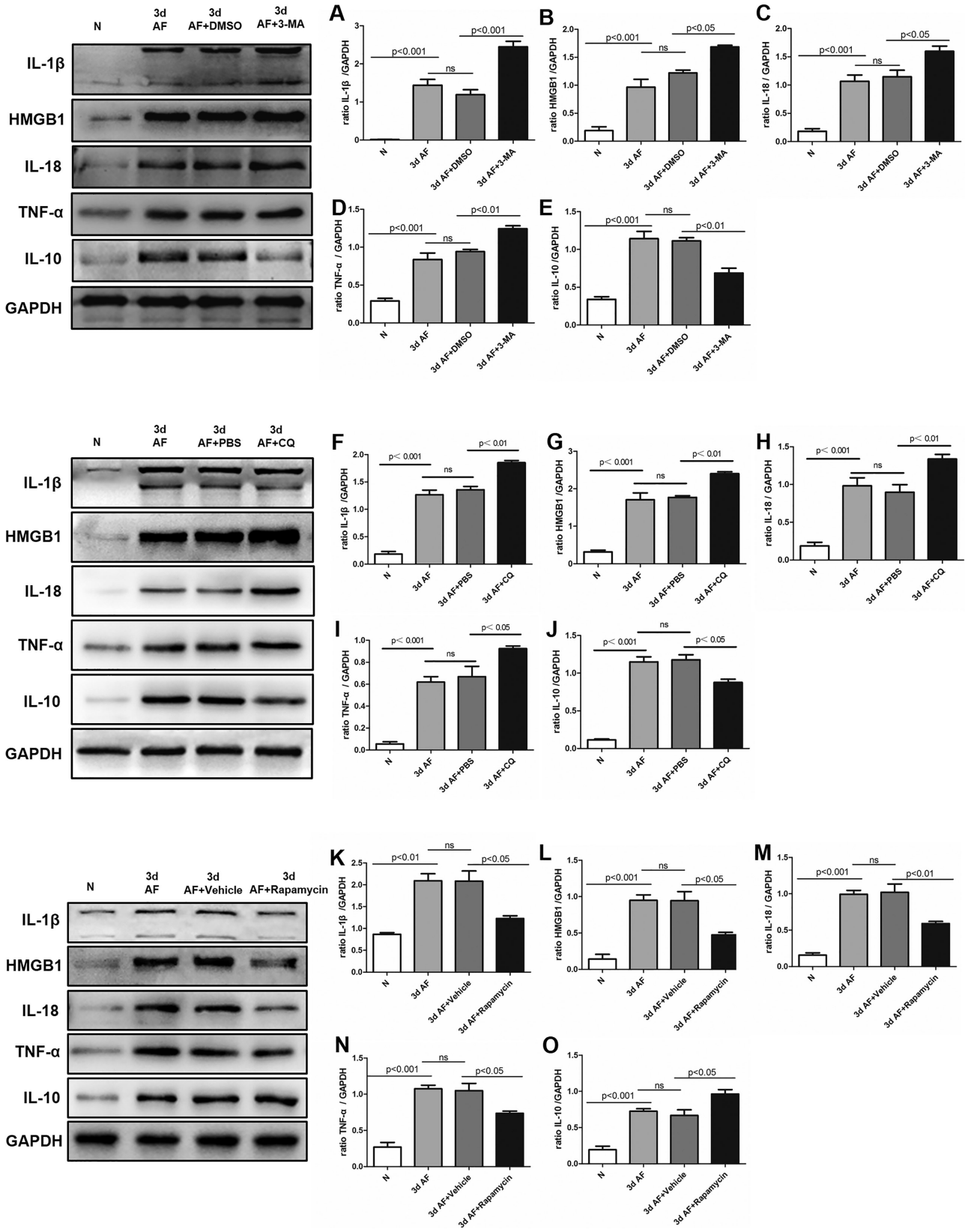

Figure 6. Effect of autophagy on inflammatory factor protein levels after *A. fumigatus* infection. (**A-E**) The protein levels of IL-1β, HMGB1, IL-18, TNF-α, and IL-10 in corneas of C57BL/6 mice after 3-MA treatment at 3 days p.i.; (**F-J**) The protein levels of IL-1β, HMGB1, IL-18, TNF-α, and IL-10 in corneas of C57BL/6 mice after CQ treatment at 3 days p.i.; (**K-O**) The protein levels of IL-1β, HMGB1, IL-18, TNF-α, and IL-10 in corneas of C57BL/6 mice after rapamycin treatment at 3 days p.i. 3-MA and CQ enhanced the expression of IL-1β, HMGB1, IL-18, and TNF-α, and reduced the level of IL-10 in corneas compared with infected control group, whereas rapamycin decreased the production of IL-1β, HMGB1, IL-18, and TNF-α, and increased the expression of IL-10 in infected corneas. Quantitation of protein levels is shown as mean ± SEM.

Investigative Ophthalmology & Visual Science

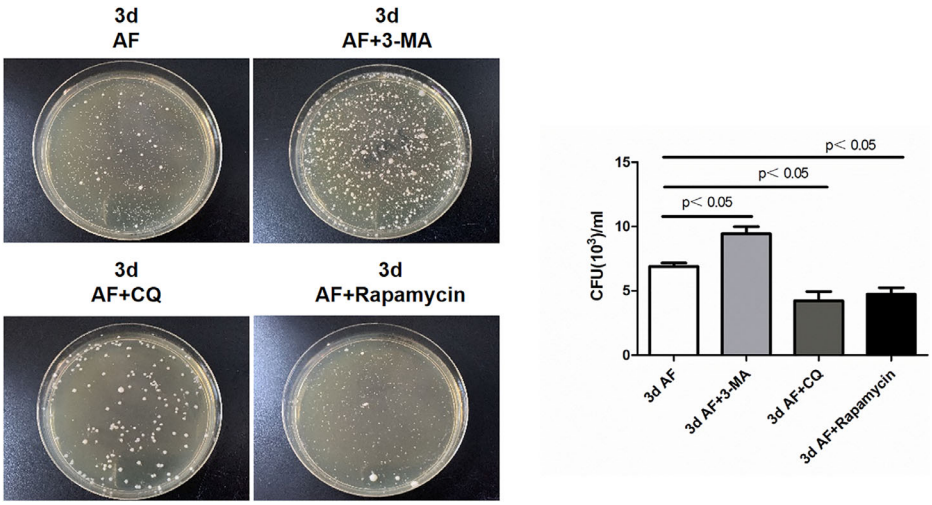

Figure 7. Effects of autophagy on fungal loads in *A. fumigatus*-infected corneas. Quantitation of fungal loads is shown as mean ± SEM. The quantification of fungal loads in corneas of mice was increased after 3-MA treatment, whereas CQ or rapamycin decreased the quantification of fungal loads compared with infected control group.

of autophagy with 3-MA and CQ significantly aggravated corneal manifestations and pathological changes when compared with infected control group, whereas disease severity was alleviated in corneas after rapamycin treatment. In addition, several groups have reported that the expression of CXCL-1 was increased after ATG5 silencing in chondrocytes, and autophagy can increase the recruitment of PMNs in lung tissue after 3-MA and CQ treatment.[31,32] Consistent with our expectation, the production of CXCL-1 and the recruitment of PMNs were markedly enhanced after autophagy inhibition compared with infected control group, whereas rapamycin treatment reduced the expression of CXCL-1 and the recruitment of PMNs, which suggested that autophagy can reduce the recruitment of PMNs in *A. fumigatus* keratitis. Interestingly, as we detected the euchromatin fraction of the nucleus and the number of granules per cytoplasm area in corneas of mice by TEM analysis, we observed that the morphology of PMNs was changed in corneas with 3-MA and CQ treatment, indicating that autophagy may play an essential role in activation, differentiation, and antibacterial ability of neutrophil. These data were consistent with studies showing that defective autophagy lead to a distinct reduction in granules and nuclear lobularization, as well as defective differentiation and dysfunction of neutrophils.[33–35]

To further determine the role of autophagy in *A. fumigatus* keratitis, the levels of inflammatory cytokines IL-1β, IL-18, HMGB1, TNF-α, and IL-10 were detected after treatment with 3-MA, CQ, and rapamycin. Results indicated that treatment with 3-MA and CQ significantly increased mRNA and protein levels of IL-1β, IL-18, HMGB1, and TNF-α, and reduced the expression of IL-10 in comparison with infected control corneas. In contrary, higher expression of IL-1β, IL-18, HMGB1, TNF-α, and lower expression of IL-10 were detected in corneas after rapamycin treatment versus infected control corneas. These data suggested that autophagy has an anti-inflammatory effect on *A. fumigatus* keratitis. Our results are consistent with studies showing that autophagy plays an important role in the defense against *Mycobacterium tuberculosis* infection in human cells.[36] Our results are also consistent with the investigations indicating that autophagy can enhance the production of IL-1β and IL-18 in response to pathogen-associated molecular patterns or LPS compared with autophagy deficient mice.[37] According to the data from animal researches, increased autophagy can mitigate the renal injury by decreasing the cytokines TNF-α, IL-6, and HMGB1, and upregulating IL-10 to balance the proinflammation and anti-inflammation responses.[38] 3-MA and CQ improve the expression of HMGB1, IL-6, and TNF-α, and decrease the production of IL-10 in acute lung injury, whereas treatment with rapamycin can downregulate the levels of HMGB1, IL-6, and TNF-α, and increase the expression of IL-10.[32]

The quantification of fungal loads in corneas of mice was increased after 3-MA treatment, whereas CQ or rapamycin decreased the quantification of fungal loads compared with infected control group. Autophagy was attenuated in corneas after being treated with 3-MA, resulting in the increased quantity of fungal loads. Conversely, rapamycin induced autophagy, leading to the amount of fungi phagocytized by autophagy increase. These results are consistent with studies that autophagy can clear intracellular pathogens and function in antigen presentation.[11] CQ interferes with the formation of autolysosome by increasing the pH in the cells. Previous studies have shown that pH also affect the growth of *A. fumigatus*,[39] which may be the cause of decreased fungal loads in our study. These three interventions are not specific to autophagy and may affect the fungal load through other pathways. Therefore further studies need to be done to explore the effects of specific interventions on autophagy on fungal loads in FK.

Conclusions

Our study demonstrates that the expression of autophagy is gradually enhanced with the progression of FK caused by *A. fumigatus*. Inhibition of autophagy aggravated the severity of *A. fumigatus* keratitis, whereas autophagy inducer alleviated the severity of keratitis via regulating the recruitment of PMNs, balancing the production of proinflammation and anti-inflammation cytokines, and possibly affecting the differentiation of neutrophils. Autophagy may play an important role in alleviating *A. fumigatus* keratitis and may

Investigative Ophthalmology & Visual Science

become a novel target for the treatment of FK. Further studies of autophagic signaling mechanisms in *A. fumigatus* keratitis of mice may deepen our understanding of the protective role of autophagy in FK.

Acknowledgments

Supported by the National Natural Science Foundation of China (No. 81470609; No. 81500695; No. 81700800; No. 81870632; No. 81800800); and the Natural Science Foundation of Shandong Province (ZR2017BH025; ZR2017MH008; ZR2013HQ007).

Disclosure: **C. Li,** None; **C. Li,** None; **J. Lin,** None; **G. Zhao,** None; **Q. Xu,** None; **N. Jiang,** None; **Q. Wang,** None; **X. Peng,** None; **G. Zhu,** None; **J. Jiang,** None

References

1. Li C, Zhao GQ, Che CY, et al. Effect of corneal graft diameter on therapeutic penetrating keratoplasty for fungal keratitis. *Int J Ophthalmol*. 2012;5:698–703.
2. Xie L, Zhong W, Shi W, Sun S. Spectrum of fungal keratitis in north China. *Ophthalmology*. 2006;113:1943–1948.
3. Maharana PK, Sharma N, Nagpal R, Jhanji V, Das S, Vajpayee RB. Recent advances in diagnosis and management of mycotic keratitis. *Indian J Ophthalmol*. 2016;64:346–357.
4. Niu Y, Zhao G, Li C, et al. *Aspergillus fumigatus* increased PAR-2 expression and elevated proinflammatory cytokines expression through the pathway of PAR-2/ERK1/2 in cornea. *Invest Ophthalmol Vis Sci*. 2018;59:166–175.
5. Peng X, Zhao G, Lin J, Li C. Interaction of mannose binding lectin and other pattern recognition receptors in human corneal epithelial cells during *Aspergillus fumigatus* infection. *Int Immunopharmacol*. 2018;63:161–169.
6. Yang Z, Klionsky DJ. Eaten alive: a history of macroautophagy. *Nature Cell Biol*. 2010;12:814–822.
7. Mizushima N, Levine B, Cuervo AM, Klionsky DJ. Autophagy fights disease through cellular self-digestion. *Nature*. 2008;451:1069–1075.
8. Feng Y, He D, Yao Z, Klionsky DJ. The machinery of macroautophagy. *Cell Res*. 2014;24:24–41.
9. Fratti RA, Backer JM, Gruenberg J, Corvera S, Deretic V. Role of phosphatidylinositol 3-kinase and Rab5 effectors in phagosomal biogenesis and mycobacterial phagosome maturation arrest. *J Cell Biol*. 2001;154:631–644.
10. Yuk JM, Shin DM, Lee HM, et al. Vitamin D3 induces autophagy in human monocytes/macrophages via cathelicidin. *Cell Host Microbe*. 2009;6:231–243.
11. Levine B. Eating oneself and uninvited guests: autophagy-related pathways in cellular defense. *Cell*. 2005;120:159–162.
12. Kanayama M, Inoue M, Danzaki K, Hammer G, He YW, Shinohara ML. Autophagy enhances NFkappaB activity in specific tissue macrophages by sequestering A20 to boost antifungal immunity. *Nat Commun*. 2015;6:5779.
13. Tam JM, Mansour MK, Khan NS, et al. Dectin-1-dependent LC3 recruitment to phagosomes enhances fungicidal activity in macrophages. *J Infect Dis*. 2014;210:1844–1854.
14. Chai P, Ni H, Zhang H, Fan X. The evolving functions of autophagy in ocular health: a double-edged sword. *Int J Biol Sci*. 2016;12:1332–1340.
15. Knöferle J, Koch JC, Ostendorf T, et al. Mechanisms of acute axonal degeneration in the optic nerve in vivo. *Proc Natl Acad Sci U S A*. 2010;107:6064–6069.
16. Okamoto T, Ozawa Y, Kamoshita M, et al. The neuroprotective effect of rapamycin as a modulator of the mTOR-NF-KB axis during retinal inflammation. *PloS One*. 2016;11:e0146517.
17. Wu TG, Wilhelmus KR, Mitchell BM. Experimental keratomycosis in a mouse model. *Invest Ophthalmol Vis Sci*. 2003;44:210–216.
18. Sun Y, Li C, Shu Y, et al. Inhibition of autophagy ameliorates acute lung injury caused by avian influenza A H5N1 infection. *Sci Signal*. 2012;5:ra16.
19. Siswantoro H, Russell B, Ratcliff A, et al. In vivo and in vitro efficacy of chloroquine against *Plasmodium malariae* and *P. ovale* in Papua, Indonesia. *Antimicrob Agents Chemother*. 2011;55:197–202.
20. Xu R, Lin J, Zhao GQ, et al. Production of interleukin-1beta related to mammalian target of rapamycin/Toll-like receptor 4 signaling pathway during *Aspergillus fumigatus* infection of the mouse cornea. *Int J Ophthalmol*. 2018;11:712–718.
21. Abdulrahman BA, Khweek AA, Akhter A, et al. Autophagy stimulation by rapamycin suppresses lung inflammation and infection by *Burkholderia cenocepacia* in a model of cystic fibrosis. *Autophagy*. 2011;7:1359–1370.
22. Borenstein A, Fine N, Hassanpour S, et al. Morphological characterization of para- and proinflammatory neutrophil phenotypes using transmission electron microscopy. *J Periodontal Res*. 2018;53:972–982.
23. Jeong J-H, Yang D-S, Koo J-H, Hwang D-J, Cho J-Y, Kang E-B. Effect of resistance exercise on muscle metabolism and autophagy in sIBM. *Med Sci Sports Exerc*. 2017;49:1562–1571.
24. Ekanayaka SA, McClellan SA, Barrett RP, Hazlett LD. Topical glycyrrhizin is therapeutic for *Pseudomonas aeruginosa* keratitis. *J Ocul Pharmacol Ther*. 2018;34:239–249.
25. Arruda DC, Matsuo AL, Silva LS, et al. Cyclopalladated compound 7a induces apoptosis- and autophagy-like mechanisms in paracoccidioides and is a candidate for paracoccidioidomycosis treatment. *Antimicrob Agents Chemother*. 2015;59:7214–7223.
26. Li T, Liu Y, Zhao J, et al. Aggravation of acute kidney injury by mPGES-2 down regulation is associated with autophagy inhibition and enhanced apoptosis. *Sci Rep*. 2017;7:10247.
27. Deretic V, Saitoh T, Akira S. Autophagy in infection, inflammation and immunity. *Nature Rev Immunol*. 2013;13:722–737.
28. Levine B, Deretic V. Unveiling the roles of autophagy in innate and adaptive immunity. *Nature Rev Immunol*. 2007;7:767–777.
29. McClung JM, McCord TJ, Ryan TE, et al. BAG3 (Bcl-2-associated athanogene-3) coding variant in mice determines susceptibility to ischemic limb muscle myopathy by directing autophagy. *Circulation*. 2017;136:281–296.
30. Samie M, Lim J, Verschueren E, et al. Selective autophagy of the adaptor TRIF regulates innate inflammatory signaling. *Nat Immunol*. 2018;19:246–254.
31. Jiang LB, Meng DH, Lee SM, et al. Dihydroartemisinin inhibits catabolism in rat chondrocytes by activating autophagy via inhibition of the NF-kappaB pathway. *Sci Rep*. 2016;6:38979.
32. Zhao H, Chen H, Xiaoyin M, et al. Autophagy activation improves lung injury and inflammation in sepsis. *Inflammation*. 2019;42:426–439.
33. Riffelmacher T, Clarke A, Richter FC, et al. Autophagy-dependent generation of free fatty acids is critical for normal neutrophil differentiation. *Immunity*. 2017;47:466–480.e5.
34. Rožman S, Yousefi S, Oberson K, Kaufmann T, Benarafa C, Simon HU. The generation of neutrophils in the bone marrow is controlled by autophagy. *Cell Death Differ*. 2015;22:445–456.
35. Jin J, Britschgi A, Schläfli AM, et al. Low autophagy (ATG) gene expression is associated with an immature AML blast

cell phenotype and can be restored during AML differentiation therapy. *Oxid Med Cell Longev*. 2018;2018:1482795.

36. Watson RO, Manzanillo PS, Cox JS. Extracellular *M. tuberculosis* DNA targets bacteria for autophagy by activating the host DNA-sensing pathway. *Cell*. 2012;150:803–815.
37. Saitoh T, Fujita N, Jang MH, et al. Loss of the autophagy protein Atg16L1 enhances endotoxin-induced IL-1beta production. *Nature*. 2008;456:264–268.
38. Ling H, Chen H, Wei M, Meng X, Yu Y, Xie K. The effect of autophagy on inflammation cytokines in renal ischemia/reperfusion injury. *Inflammation*. 2016;39:347–356.
39. Henriet SS, Jans J, Simonetti E, et al. Chloroquine modulates the fungal immune response in phagocytic cells from patients with chronic granulomatous disease. *J Infect Dis*. 2013;207:1932–1939.

Investigative Ophthalmology & Visual Science